Estimation of Equivalent Model of Photovoltaic Array Using Unscented Kalman Filters

M. A. González-Cagigal, José A. Rosendo-Macías, and A. Gómez-Expósito, *Life Fellow*, *IEEE*

***Abstract*—This paper proposes the use of the unscented Kalman filter to estimate the equivalent model of a photovoltaic (PV) array, using external measurements of current and voltage at the inverter level. The estimated model is of interest to predict the power output of PV plants, in both planning and operation scenarios, and thus improves the efficient operation of power systems with high penetration of renewable energy. The proposed technique has been assessed in several simulated scenarios under different operating conditions. The results show that accurate estimates are provided for the model parameters, even in the presence of measurement noise and abrupt variations under the external conditions.**

***Index Terms*—Equivalent model, parameter estimation, photovoltaic energy, unscented Kalman filter.**

I. Introduction

In many countries, solar energy is becoming one of the main sources of renewable energy. Photovoltaic (PV) technology has been widely adopted due to its high reliability, simplicity, low upfront and maintenance costs, and low environmental impact [1]. However, the efficiency of a PV system is highly dependent on environmental factors such as solar irradiation [2], temperature [3], and maintenance (i.e., cleaning) routines [4], which can significantly affect the performance of the overall system. In this regard, the optimal operation of PV systems benefits from an accurate modeling of PV modules, including the identification of parameters involved in the mathematical model [5].

Several methods have been proposed for the estimation of PV model parameters, which can be broadly grouped into: analytical methods [6], [7], where manufacturer data are directly used to calculate the parameter values based on explicit expressions; metaheuristic methods, where the identification of parameters is formulated as an optimization problem [8], [9]; and hybrid methods, where the advantages of the two previous methods are combined [10].

All of these techniques address the parameter estimation problem in a static fashion. However, the temperature of PV panels, which evolves over time according to a series of well-known heat transfer mechanisms, has a remarkable influence on the power delivered by the system. For this reason, dynamic state estimators (DSEs) can be the right tool for a joint estimation of the state variables and parameters involved in the modelling of PV modules. The most common formulation of DSEs resorts to Kalman filters (KFs), which are widely used for state estimation in electric power systems [11], and also for parameter identification [12], [13].

A particular formulation of the KF, the so-called unscented KF (UKF), has gained popularity due to its good performance in the estimation of non-linear systems, compared to other formulations such as the extended KF (EKF) [14].

When real PV power plants are analyzed, though, composed of arrays of PV panels connected in series, the estimation of parameters at the module level can be difficult in terms of computational complexity and lack of required individual measurements. To overcome this issue, this paper proposes a UKF-based estimation technique for the identification of states and parameters of an equivalent model of a PV array, using measurements of the terminal voltage and current along with the information provided by weather stations. The proposed implementation of the UKF solves an implicit equation for the output current, without the need to calculate the Jacobian matrices for the state transition and observation models. The complexity involved in computing these matrices hampers the application of the EKF formulation to the problem at hand.

The proposed technique is validated using different simulation scenarios, showing the benefits of the estimation technique when planning the maintenance of PV panels and obtaining a prediction of the energy produced by the array. Moreover, the identification of the equivalent model of a PV array can enhance the operation and control of the overall power system. To the authors' best knowledge, there has been no research attempting to estimate an equivalent model for a PV array, taking into account the dynamic evolution of the panel temperature, based on the produced power and external conditions.

In a preliminary work [15], the authors applied the UKF to the joint state and parameter estimation of PV modules. The main contributions of this paper with respect to [15] are as follows.

1) The proposed estimation technique is applied to the identification of parameters of an equivalent model, corresponding to a whole PV array, while in [15], the estimated

Manuscript received: July 26, 2023; revised: October 17, 2023; accepted: November 20, 2023. Date of CrossCheck: November 20, 2023. Date of online publication: December 12, 2023.

M. A. González-Cagigal (corresponding author), J. A. Rosendo-Macías, and A. Gómez-Expósito are with the Department of Electrical Engineering, University of Seville, Spain, and A. Gómez-Expósito is also with ENGREEN Laboratory of Engineering for Energy and Environmental Sustainability, Seville, Spain (e-mail: mgcagigal@us.es; rosendo@us.es; age@us.es).

DOI: 10.35833/MPCE.2023.000510

model was for a single PV panel.

2) The panel temperature was assumed to have an unknown dynamic evolution [15]. In this work, a thermal model is considered for such an important variable in the electricity performance of a PV facility.

3) Many more and more comprehensive tests have been designed in this paper to check the suitability of the UKF for this purpose.

The remainder of this paper is organized as follows. Section II presents the UKF algorithm, while the equivalent model of the PV module is described in Section III. The implementation of the UKF-based estimation technique to the system under study is provided in Section IV. The case studies used to assess the performance of the UKF-based estimation technique and the application of this technique to energy management are addressed in Sections V and VI, respectively. Section VII outlines the main conclusions.

II. UKF Algorithm

KF implementations require a set of state equations, including the dynamic and measurement equations. In the case of continuous-time and discrete-measurement non-linear systems, these equations can be expressed as:

$$\dot{\boldsymbol{x}}(t)=\boldsymbol{f}(\boldsymbol{x}(t),\boldsymbol{u}(t))+\boldsymbol{w}(t) \tag{1}$$

$$\boldsymbol{z}(t_k)=\boldsymbol{g}(\boldsymbol{x}(t_k),\boldsymbol{u}(t_k))+\boldsymbol{v}(t_k) \tag{2}$$

where $\boldsymbol{x}(t)$ is the state vector; $\boldsymbol{u}(t)$ is the system input vector; $\boldsymbol{z}(t_k)$ is the measurement vector at instant t_k; $\boldsymbol{f}(\cdot)$ and $\boldsymbol{g}(\cdot)$ are the measurement functions; and $\boldsymbol{w}(t)$ and $\boldsymbol{v}(t_k)$ are the model and measurement noises, which are assumed Gaussian processes with covariance matrices $\boldsymbol{Q}$ and $\boldsymbol{R}$, respectively.

In the discrete time domain, considering a time step Δt, the above equations become:

$$\boldsymbol{x}_k=\boldsymbol{x}_{k-1}+\Delta t\boldsymbol{f}(\boldsymbol{x}_{k-1},\boldsymbol{u}_{k-1})+\boldsymbol{w}_k \tag{3}$$

$$\boldsymbol{z}_k=\boldsymbol{g}(\boldsymbol{x}_k,\boldsymbol{u}_k)+\boldsymbol{v}_k \tag{4}$$

From the above discrete model, by linearizing the non-linear functions in (3) and (4), the EKF can be readily applied. However, in the particular application considered in this work, implicit equations are involved in the observation model, so the calculation of the Jacobian matrices for functions $\boldsymbol{f}(\cdot)$ and $\boldsymbol{g}(\cdot)$ is far from trivial. For this reason, this work makes use of the UKF, whose implementation is based on an iterative process with two different stages [16].

A. Prediction Stage

At instant k, a cloud of $2L+1$ vectors, called σ-points, is calculated from the previous estimate of the state vector $\hat{\boldsymbol{x}}_{k-1}$ (dimension L) and the covariance matrix of the state estimation error $\boldsymbol{P}_{k-1}$ using the following expression:

$$\begin{cases}\boldsymbol{x}_{k-1}^{0}=\hat{\boldsymbol{x}}_{k-1}\\ \boldsymbol{x}_{k-1}^{i}=\hat{\boldsymbol{x}}_{k-1}+\left[\sqrt{(L+\lambda)\boldsymbol{P}_{k-1}}\right]_i & i=1,2,...,L\\ \boldsymbol{x}_{k-1}^{i+L}=\hat{\boldsymbol{x}}_{k-1}-\left[\sqrt{(L+\lambda)\boldsymbol{P}_{k-1}}\right]_{i+L} & i=1,2,...,L\end{cases} \tag{5}$$

where $\left[\sqrt{(L+\lambda)\boldsymbol{P}_{k-1}}\right]_i$ is the i^{th} column of the matrix $\sqrt{(L+\lambda)\boldsymbol{P}_{k-1}}$ that has been calculated in this work using the Cholesky decomposition; and λ is a scaling factor calculated from (6).

$$\lambda=\alpha_{\text{f}}^2(L+\kappa)-L \tag{6}$$

where α_{f} and κ are the filter parameters to be tuned. These σ-points, evaluated using (3), yield $2L+1$ vectors $\boldsymbol{x}_k^{i-}$, from which the a priori estimations $\hat{\boldsymbol{x}}_k^-$ and $\boldsymbol{P}_k^-$ are obtained as:

$$\hat{\boldsymbol{x}}_k^-=\sum_{i=0}^{2L}W_{mi}\boldsymbol{x}_k^{i-} \tag{7}$$

$$\boldsymbol{P}_k^-=\sum_{i=0}^{2L}W_{ci}(\boldsymbol{x}_k^{i-}-\hat{\boldsymbol{x}}_k^-)(\boldsymbol{x}_k^{i-}-\hat{\boldsymbol{x}}_k^-)^{\text{T}}+\boldsymbol{Q}_k \tag{8}$$

where W_{mi} and W_{ci} are the elements of the weighting vectors $\boldsymbol{W}_m$ and $\boldsymbol{W}_c$, respectively, which are calculated as (9).

$$\begin{cases}W_{m0}=\dfrac{\lambda}{L+\lambda}\\ W_{c0}=\dfrac{\lambda}{L+\lambda}+1-\alpha_{\text{f}}^2+\beta\\ W_{mi}=W_{ci}=\dfrac{1}{2(L+\lambda)} & i=1,2,...,2L\end{cases} \tag{9}$$

where β is another tunable parameter.

B. Correction Stage

On the basis of the a priori estimations, a new cloud of vectors is calculated as:

$$\begin{cases}\boldsymbol{x}_k^{0-}=\hat{\boldsymbol{x}}_k^-\\ \boldsymbol{x}_k^{i-}=\hat{\boldsymbol{x}}_k^-+\left[\sqrt{(L+\lambda)\boldsymbol{P}_k^-}\right]_i & i=1,2,...,L\\ \boldsymbol{x}_k^{(i+L)-}=\hat{\boldsymbol{x}}_k^--\left[\sqrt{(L+\lambda)\boldsymbol{P}_k^-}\right]_{i+L} & i=1,2,...,L\end{cases} \tag{10}$$

Formula (10) is then used to evaluate the measurement function $\boldsymbol{g}(\cdot)$ in (4), yielding

$$\boldsymbol{\gamma}_k^{i-}=\boldsymbol{g}(\boldsymbol{x}_k^{i-},\boldsymbol{u}_k)\quad i=0,1,...,2L \tag{11}$$

These values are weighted using W_{mi} defined by (9) as:

$$\hat{\boldsymbol{z}}_k^-=\sum_{i=0}^{2L}W_{mi}\boldsymbol{\gamma}_k^{i-} \tag{12}$$

Then, the covariance matrix of the measurement estimation error $\boldsymbol{P}_{zk}^-$ and the cross-covariance matrix of state and measurements $\boldsymbol{P}_{xzk}^-$ are obtained using W_{ci} as follows:

$$\boldsymbol{P}_{zk}^-=\sum_{i=0}^{2L}W_{ci}(\boldsymbol{\gamma}_k^{i-}-\hat{\boldsymbol{z}}_k^-)(\boldsymbol{\gamma}_k^{i-}-\hat{\boldsymbol{z}}_k^-)^{\text{T}}+\boldsymbol{R}_k \tag{13}$$

$$\boldsymbol{P}_{xzk}^-=\sum_{i=0}^{2L}W_{ci}(\boldsymbol{x}_k^{i-}-\hat{\boldsymbol{x}}_k^-)(\boldsymbol{\gamma}_k^{i-}-\hat{\boldsymbol{z}}_k^-)^{\text{T}} \tag{14}$$

By using the a priori estimations at instant k from (7) and (8) and the Kalman gain from (15), the a posteriori estimations can be obtained from (16) and (17), respectively, both of which are necessary for the next step.

$$\boldsymbol{K}_k=\boldsymbol{P}_{xzk}^-(\boldsymbol{P}_{zk}^-)^{-1} \tag{15}$$

$$\hat{\boldsymbol{x}}_k=\hat{\boldsymbol{x}}_k^-+\boldsymbol{K}_k(\boldsymbol{z}_k-\hat{\boldsymbol{z}}_k^-) \tag{16}$$

$$\boldsymbol{P}_k=\boldsymbol{P}_k^-\boldsymbol{K}_k\boldsymbol{P}_{zk}^-\boldsymbol{K}_k^{\text{T}} \tag{17}$$

C. Parameter Estimation

State estimation requires the previous knowledge of the parameters involved in the dynamic model, such as that presented in the following section for the equivalent model of PV module. However, when these parameters are not known, estimation techniques such as UKF can be used for a joint estimation of state variables and parameters [17]. In this way, an augmented state vector $\boldsymbol{x}_a^{\mathrm{T}}=[\boldsymbol{x}^{\mathrm{T}},\boldsymbol{\psi}^{\mathrm{T}}]$ is adopted, where $\boldsymbol{x}$ contains the state variables and $\boldsymbol{\psi}$ includes the model parameters to be identified. Then, the dynamic model represented by (3) and (4) is replaced by the augmented one:

$$\begin{bmatrix}\boldsymbol{x}_k\\ \boldsymbol{\psi}_k\end{bmatrix}=\begin{bmatrix}\boldsymbol{x}_{k-1}+\Delta t\boldsymbol{f}(\boldsymbol{x}_{k-1},\boldsymbol{u}_{k-1})\\ \boldsymbol{\psi}_{k-1}\end{bmatrix}+\boldsymbol{w}_k \tag{18}$$

$$\boldsymbol{z}_k=\boldsymbol{g}(\boldsymbol{x}_{ak},\boldsymbol{u}_k)+\boldsymbol{v}_k \tag{19}$$

where $\boldsymbol{w}_k$ is now the augmented model noise vector, including not only the state variable components, but also the parameter components.

III. Equivalent Model of PV Module

In this section, the equivalent model considered for the PV module is presented, as implemented in the UKF algorithm previously described. A single-diode model is taken, as presented in [18] and represented in Fig. 1.

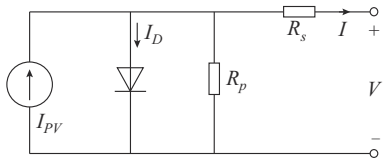

Fig. 1. Single-diode model considered for equivalent model of PV module.

The current through the diode I_D is calculated using the Shockley's equation as:

$$I_D=I_n\left(\exp\left(\frac{q(V+R_sI)}{AN_skT}\right)-1\right) \tag{20}$$

where I_n is the reverse bias saturation current of the diode; A is the diode ideality factor; N_s is the number of cells connected in series; k is the Boltzmann constant; V is the terminal voltage of the equivalent model of PV module; q is the electron charge; R_s is the series resistance; I is the terminal current of the equivalent PV module; and T is the temperature of the equivalent model.

The current produced by the equivalent model of PV module I_{PV} in Fig. 1 is obtained using the array irradiation G_{PV} and the average array temperature, yielding the following expression.

$$I_{PV}=\frac{G_{PV}}{G^{ref}}[I_L^{ref}+\mu(T-T^{ref})] \tag{21}$$

where G^{ref} is the reference irradiation; T^{ref} is the reference temperature; μ is the temperature coefficient; and I_L^{ref} is the short-circuit current of the module under standard conditions. The value of G_{PV} depends on the solar irradiation G_s and a so-called cleaning factor, denoted as c and used in [15]. This factor is determined by the soiling of panels comprising the array for which the equivalent model is estimated. Taking the above into account, the following expression is considered for G_{PV}:

$$G_{PV}=cG_s \tag{22}$$

Finally, I is calculated through Kirchhoff's current law as follows:

$$I=I_{PV}-I_D-\frac{V+R_sI}{R_p} \tag{23}$$

where R_p is the parallel resistance.

It can be noticed that the model represented by (20)-(23) is algebraic and the parameters involved are considered as constants. However, it is well known that the temperature of the PV panels evolves dynamically according to the thermal equilibrium equation, derived from the first law of thermodynamics, yielding:

$$C_m\frac{\mathrm{d}T}{\mathrm{d}t}=\alpha Q_s-P-Q_c-Q_r \tag{24}$$

where C_m is the heat capacity of the equivalent model of PV module; Q_s is the array heating by solar radiation; α is the absorption factor of PV cells; P is the power produced by the array ($P=VI$); Q_c is the conductive heat transfer; and Q_r is the radiative heat transfer. For the last two terms, the expressions in [19] are used in the case study presented in this paper. The values of Q_s, Q_c, and Q_r depend on the following meteorological variables: ambient temperature T_{amb}, solar radiation G_s, and and horizontal wind speed v_w (in this work, the PV panels are assumed to be in horizontal position for the test cases presented in Section V).

The magnitudes of those variables can be collected by weather stations located at the corresponding PV plant.

Regarding the absorption factor α, [20] presents an experimental analysis concluding that 90.5% is an adequate value for this parameter in crystalline silicon PV cells, so that $\alpha=$ 0.905 p.u. will be considered in this work.

From (24), it is concluded that the temperature of the equivalent model of PV module at instant k is dependent on its value at instant $k-1$, which leads naturally to a DSE model aimed at jointly estimating the state variables and the model parameters.

IV. Implementation of UKF-based Estimation Technique

The implementation of the proposed UKF-based estimation technique is depicted in the flowchart of Fig. 2.

A. Data Acquisition and Estimation of Equivalent Model of PV Module

As mentioned in Section II, an augmented state vector can be defined when the model parameters are not known, so that a joint estimation can be carried out using the UKF. For the equivalent model of PV module described in Section III, the state vector $\boldsymbol{x}$ is only composed of the temperature of the equivalent model:

$$\boldsymbol{x}=[T] \tag{25}$$

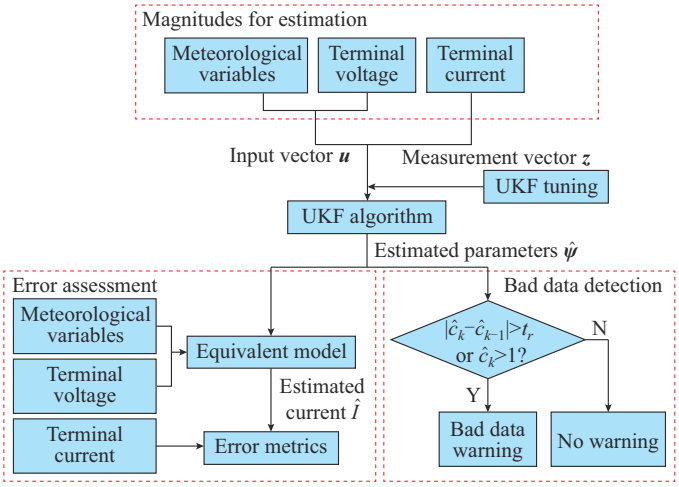

Fig. 2. Flowchart of proposed UKF-based estimation technique.

While the components of the parameter vector $\boldsymbol{\psi}$ are:

$$\boldsymbol{\psi}^{\mathrm{T}}=[R_s \quad R_p \quad \mu \quad A \quad c] \tag{26}$$

So, the size of the augmented state vector $\boldsymbol{x}_a$ is $L=6$. In the implementation of the proposed technique, a total of 5 magnitudes are supposed to be measured from the system under study, namely the terminal voltage V and current I, together with the meteorological variables presented in Section III. These magnitudes are divided into system inputs, yielding the vector $\boldsymbol{u}^{\mathrm{T}}=[V, T_{amb}, G_s, v_w]$ and the measurements used in the correction stage of the estimator $\boldsymbol{z}=[I]$ [21].

The state-transition equation (3) in the UKF algorithm is as follows:

$$T_k=T_{k-1}+\frac{\Delta t}{C_m}(\alpha Q_{s,k-1}-V_{k-1}I_{k-1}-Q_{c,k-1}-Q_{r,k-1}) \tag{27}$$

where $Q_{c,k-1}$ and $Q_{r,k-1}$ are calculated using the expressions in [19], the panel temperature, the wind speed, and the ambient temperature at instant $k-1$.

Regarding the measurement function $\boldsymbol{g}(\cdot)$ in (11), it is not possible to obtain an explicit expression for the current I, as a function of the state variable and system inputs. For this reason, the corresponding implicit equation has to be solved:

$$I_k=\frac{c_k G_{s,k}}{G^{ref}}[I_L^{ref}+\mu_k(T_k-T^{ref})]- I_n\left(\exp\left(\frac{q(V_k+R_{s,k}I_k)}{A_k N_s k T_k}\right)-1\right)-\frac{V_k+R_{s,k}I_k}{R_{p,k}} \tag{28}$$

The specific details related to the UKF tuning will be provided in the following section.

B. Error Assessment

After estimating the parameters of the equivalent model, it is crucial to assess the reliability of the estimate. For this purpose, an additional set of data is generated for the simulated system under study. Then, this test set is used to verify whether the terminal current predicted by the reduced estimated model aligns well with the current measured from the entire PV array. In this regard, several metrics will be explored in Section V to evaluate the accuracy of the estimated model.

Additionally, a comparison will be presented between the results provided by the proposed technique and the EKF scheme [22]. The analytical derivation of the required Jacobian matrix for $\boldsymbol{g}(\cdot)$ is far from trivial, given the implicit nature of this function. To overcome this issue, numerical methods should be used for the derivation of this Jacobian matrix. However, as standard methods gave rise to numerical problems, a robust technique based on complex-step differentiation [23] is finally adopted in this work for the EKF scheme.

C. Bad Data Detection

As stated in Section III, the estimated cleaning factor c is intended to quantify the level of soiling of the array of PV panels. However, sudden variations in this parameter could originate from bad data in the measurements of solar radiation or terminal current. To address this issue, two verifications concerning the estimated value of c are proposed at each time step.

1) Absolute deviations in the estimated value of c from instant $k-1$ to k, i.e., $|\hat{c}_k-\hat{c}_{k-1}|$, exceeding a specific threshold (t_r in Fig. 2) might be caused either by abrupt variations in the cleaning factor or by bad data in the involved measurements, so that a warning notification should be triggered. This allows for an analysis of the underlying cause behind this sudden variation.

2) Considering the nature of the cleaning factor, an estimation where $\hat{c}_k>1$ should be regarded as an indicator of bad data.

The points described above focus on detecting and eventually identifying permanent outliers. The impact of sporadic (i.e., non-permanent) inaccurate data on the accuracy of the estimated model is evaluated in the following section.

V. Case Studies

In this section, the proposed technique is assessed in its ability to estimate the state and parameters of an equivalent model for a PV array composed of 16 modules, as shown in Fig. 3, where the terminal voltage and current measurements are represented. Three scenarios are considered in this paper. For the calculation of the terminal voltage of the PV array in the simulation, a maximum power point tracker is implemented in the inverter, based on a perturb and observe method [24].

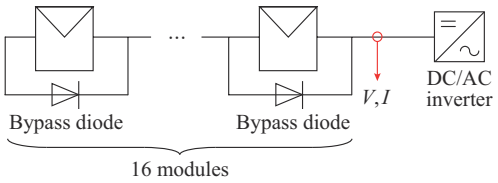

Fig. 3. PV array considered in case studies.

In all the scenarios included in this paper, commercial 180 W PV modules are considered, characterized by the data shown in Table I [25]. In order to emulate the natural manufacturing variability of these parameters for the set of modules comprising the array, 10% random errors have been added to the values of R_s, R_p, A, μ, and I_n in Table I. The men-

tioned variability further justifies the use of UKF for the estimation of parameters in the equivalent model, since the real values of parameters of the 16 modules are unknown.

TABLE I
PARAMETERS OF TESTED PV MODULES

Parameter	Value
R_s	0.39381 Ω
R_p	313.055 Ω
A	0.98119
μ	0.0032 A/K
N_s	60
I_n	10^{-9} A
I_L^{ref}	7.34 A
Length	1.576 m
Width	0.825 m
Weight	22.7 kg
Rated power	180 W

The UKF requires an initial estimation of the augmented state vector. For this purpose, the panel temperature is initialized in all cases with the measured ambient temperature value at the beginning of the simulation, while the parameters of the equivalent model are given the values included in Table I. Regarding the covariance of this estimation error, it is initialized as a diagonal matrix, namely

$$\boldsymbol{P}_0 = diag(1, 1, 1, 1, 1, 1) \tag{29}$$

The UKF is implemented considering the parameters $\alpha = 10^{-4}$, $\kappa = 3 - L = -4$, and $\beta = 2$, as proposed in [26], where the influence of these scaling parameters is assessed. The covariance of the measurement noise is taken as a diagonal matrix with $R_{ii} = 10^{-4}$. Finally, for the model noise covariance matrix $\boldsymbol{Q}$, a self-tuning process is implemented, as proposed in [27], where $\boldsymbol{Q}$ is estimated as the innovation covariance.

The proposed technique is assessed in a scenario where the whole set of parameters is estimated under normal operating conditions. Once the model parameters are identified, two additional scenarios are presented where only the coefficient c is included in the augmented state vector for the UKF algorithm, while the rest of the parameters are given their estimated values in the first scenario.

In all scenarios, MATLAB has been used for the simulation of the complete PV array and the implementation of the proposed technique. To conduct the case studies in this work, a computer with an Intel(R) Core(TM) i5-8400 CPU running the Windows 10 Pro OS is used. As a reference, the computation time in the first scenario (with information from 5 hours) for the proposed technique is 10.37 s.

A. Scenario I: Normal Operation

In scenario I, typical profiles for the solar irradiance and the ambient temperature are assumed, as represented in Fig. 4 for the 10 hours considered in the simulation. A time step $\Delta t = 1$ min is chosen, with 1% error artificially added to the measured magnitudes.

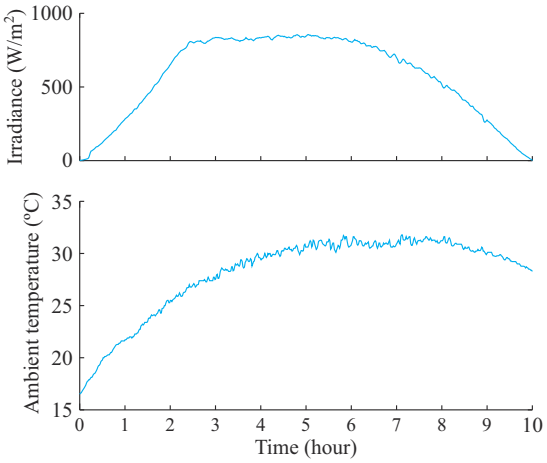

Fig. 4. Solar irradiance and ambient temperature in scenario I.

For the cleaning factor of the PV modules, a baseline value $c = 0.85$ p.u. with 10% random error is used in the simulation. A typical profile has also been considered for the wind speed variation, so that the dynamic evolution of the panel temperatures can be obtained and, as a byproduct, the terminal voltage of the simulated PV array can be obtained.

Using the measurements from the first 5 hours of the simulation, the UKF provides the estimated parameters in the equivalent model shown in Fig. 5. Additionally, the simulated temperatures of the 16 modules in the array are shown in Fig. 6 (solid lines), along with the estimated temperature of the equivalent model of the PV panel (dashed line). It can be noticed that the estimated temperature lies in the middle of the simulated temperatures, as expected.

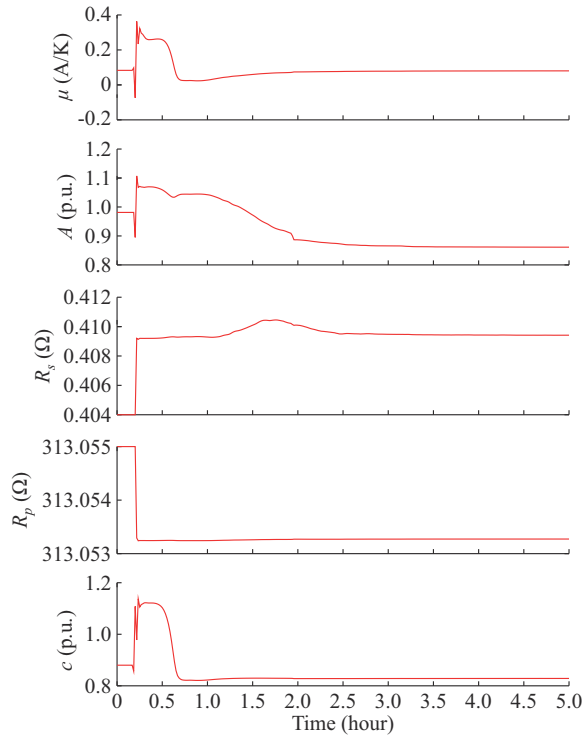

Fig. 5. Estimated parameters in scenario I.

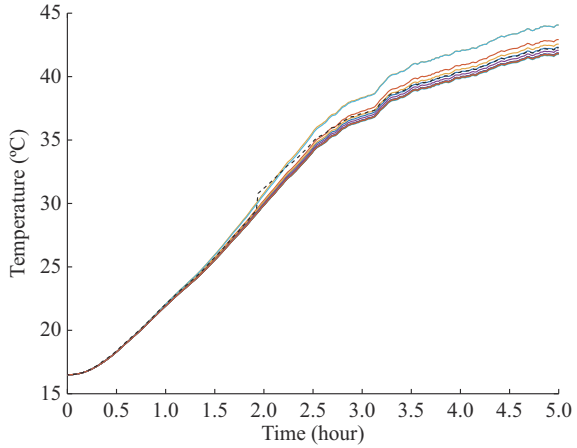

Fig. 6. Simulated temperatures of PV modules and estimated temperature of equivalent PV panel.

The EKF formulation was also considered in this scenario for the estimation of equivalent parameters. As mentioned previously, a numerical calculation of Jacobian matrices is implemented, using a complex-step differentiation method. Despite the use of this sophisticated tool, the EKF presents slower convergence speed in the parameter estimation compared with that of the UKF, as depicted in Fig. 7 for the series resistance R_s, where it can be observed that a steady-state value is not reached in the case of the EKF for the considered time lapse.

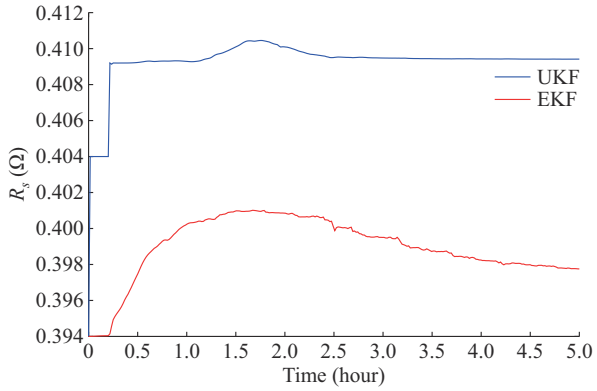

Fig. 7. Estimation of parameter R_s provided by EKF and UKF.

In order to assess the accuracy of the estimated parameters, the evolution of the actual (i.e., simulated) terminal current during the last 5 hours of the simulation is compared to the terminal currents calculated with the equivalent model considering estimated parameters provided by the UKF (model 1) or EKF (model 2) and the equivalent model considering baseline parameters assumed in Table I (model 3). This comparison is represented in Fig. 8, where it can be noticed that the terminal current calculated with model 1 is much closer to the simulated one, giving evidence of the good performance of the proposed technique. Additionally, the terminal current calculated with model 2 is clearly less accurate than that calculated with model 1.

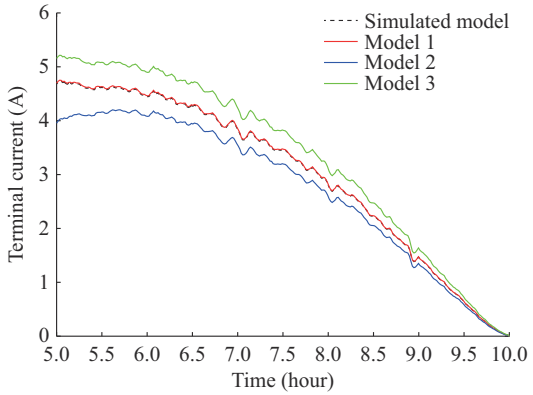

Fig. 8. Comparison of simulated and calculated terminal currents.

To quantify the resulting errors in the calculated terminal current, the mean relative error (MRE), the mean square error (MSE), and the maximum absolute error (MAE) are presented in Table II for models 1-3. As previously mentioned, the errors obtained with model 1 are lower than those obtained with models 2 and 3.

TABLE II
METRICS OF OBTAINED ERRORS IN TERMINAL CURRENT

Model	MRE (%)	MSE (A^2)	MAE (A)
1	1.49	0.14	0.06
2	5.61	0.92	0.73
3	6.77	1.12	0.48

The influence of the measurement errors in the accuracy of the estimated model is subsequently analyzed. Table III shows the MRE of the calculated terminal current with different noise levels in measurements within the same time lapse as in Fig. 8. It can be noticed that, even for high noise levels in the measurements, the resulting MRE remains acceptable, showing that the proposed technique is robust against high measurement errors.

TABLE III
MRE OF CALCULATED TERMINAL CURRENT WITH DIFFERENT NOISE LEVELS IN MEASUREMENTS

Noise level (%)	MRE (%)
1	1.49
2	1.58
5	3.02
7	6.85

Finally, the performance of the proposed technique is assessed when measurements of the terminal current sporadically contain outliers (bad data). In this context, Table IV shows the MREs in the terminal current with the increasing rate of outliers. The outliers are created by randomly setting the measured values to be 10 or 0.1 times the corresponding simulated values. In light of the results presented in Table IV, it can be concluded that the deterioration of the UKF per-

formance is not very pronounced when reasonable rates of outliers are considered. Furthermore, to attenuate the potential impact of outliers, a pre-processing of the database used for the estimation could be implemented to detect and remove outliers.

TABLE IV
MRE IN TERMINAL CURRENT WITH INCREASING RATE OF OUTLIERS

Rate of outliers (%)	MRE (%)
1	1.51
2	1.97
5	4.72

B. Scenario II: Global Variation in Cleaning Factor

In this scenario, abrupt changes in the cleaning factor c are simultaneously applied to the 16 modules in the PV system under study. First, at the 3rd hour, all cleaning factors are reduced 60% of their initial values, simulating a sudden soiling of panels. This may happen, for instance, when a flock of sheep runs in the vicinity of a PV plant, an increasingly common situation in certain rural areas, also, after a dust or sand storm in desert areas. Then, at the 6th hour, these values are increased to $c=1$ p. u., assuming that the modules have been cleaned (for example, due to the effect of rain). In this scenario, only the coefficient c is included in the parameter vector to be estimated, and the external conditions are equal to those in that scenario.

Figure 9 represents the evolution of the coefficient c in the equivalent model of the PV module. It can be noticed that this parameter decreases at the 3rd hour and increases at the 6th hour, giving evidence of the good performance of the proposed technique.

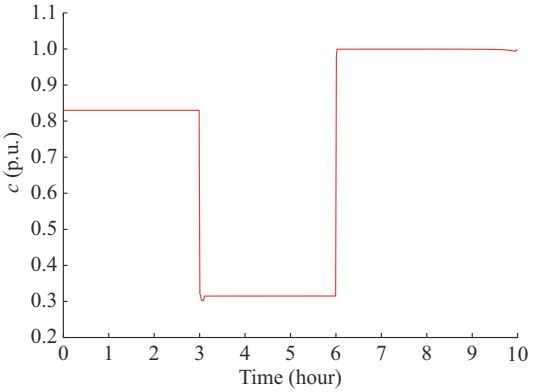

Fig. 9. Estimation of parameter c in scenario II.

The ability demonstrated by the proposed technique to detect sudden or long-term variations in the production of a PV array, due for example to a sustained soiling of panels, can be exploited for the development of suitable PV plant maintenance routines.

C. Scenario III: Partial Reduction of Cleaning Factor

In scenario II, the parameter c is simultaneously changed for the whole set of modules in the PV array, assuming all panels in series are affected by the same natural phenomena. However, in certain situations, only a reduced number of panels are affected by bird droppings (most common) or soiling, and the resulting change in the power production can be mistaken for normal variations under the external conditions, or even with measurement errors.

To assess this issue, scenario III analyzes the estimation of the parameter c in the equivalent model of the PV module under partial soiling conditions or panel malfunctioning. For the subset of affected panels, the simulated cleaning factor is set to be the extreme value $c=0$ from the 5th hour until the end of the simulation. As in scenario II, the parameters have been given their estimated values in scenario I. Figure 10 represents the estimated values of cleaning factor c when 1, 3, and 5 modules are affected by the sudden cleaning decrease.

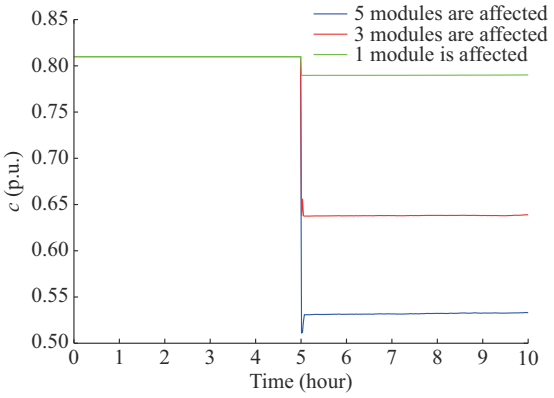

Fig. 10. Estimation of parameter c in scenario III.

In all cases, the estimation of c remains essentially constant until the event occurs. In all cases with modules affected by soiling or malfunctioning, the proposed technique succeeds in detecting the associated decrease in the parameter c of the equivalent model.

Based on the aforementioned results, it can be concluded that the proposed technique allows the identification of situations in which a small subset of modules in a particular array have stopped producing energy. This aspect is not only important from the point of view of energy production, but also for maintenance purposes, as these undesired operating conditions can lead to hot spots that can shorten the life of assets.

VI. APPLICATION TO PRODUCTION MANAGEMENT

In the previous section, the proposed technique has been assessed in the identification of the equivalent model of a PV array under different external conditions. In this section, the dynamically updated values of these parameters will be used to enhance the predicted values of the energy produced by the array.

In this case, 15-min prediction intervals are considered for meteorological variables. The 10-hour predicted output energy is represented in Fig. 11 for the simulated model of the PV array and models 1 and 3 in scenario I.

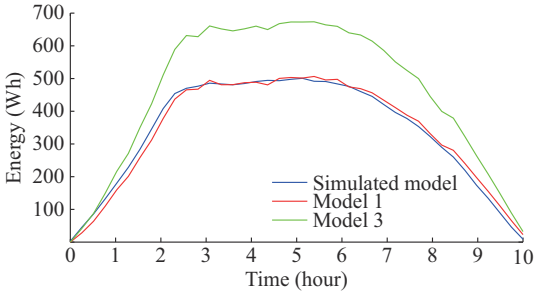

Fig. 11. Comparison of predicted output energy.

It can be noticed that the values obtained by model 1 are much closer to those of the simulated model than the ones obtained by model 3, giving evidence of the accuracy of the proposed technique. The 10-hour prediction can be recalculated in real time as the estimated values of the parameters are updated using the corresponding measurements. The enhanced predictions could be used, for instance, in the operation scheduling of battery energy storage systems associated to large-scale or rooftop PV power plants.

VII. Conclusion

In this paper, a novel technique is presented for the state estimation and parameters of an equivalent model of a PV array, using for the unscented formulation of the KF. The use of the proposed technique is motivated by the dynamic behavior of the temperature of PV panels, which has a remarkable influence on the power production. The equivalent model considered is based on a PV module with a single-diode model. For the joint estimation, a set of external measurements are used, including not only electrical variables such as the terminal current and voltage, but also the meteorological conditions affecting the thermal model of panels. Four simulated scenarios have been considered in this work in order to evaluate the performance of the proposed technique.

The proposed technique is assessed with normal operating conditions, where it shows its ability to estimate an equivalent dynamic model of the PV array, which accurately calculates the terminal DC current. The proposed technique can also provide acceptable results, both when measurements with larger average errors are considered and in the presence of temporary outliers. Additionally, the proposed technique is compared to the EKF formulation. It can be concluded that the latter formulation has lower accuracy in the estimation of the equivalent model, compared to the proposed technique.

In a second scenario, a global decrease in the cleaning coefficient is simulated, and the proposed technique is able to detect this variation in the corresponding parameter of the equivalent model. Then, a third scenario is aimed at assessing if the proposed technique can identify situations when only a reduced number of modules in the PV array are affected by soiling or malfunctioning. The results show that even if 10%-15% of the modules in an array stop producing electricity, the proposed technique can detect this anomalous condition by noticeable deviations in the equivalent cleaning factor, which can be helpful for prematurely detecting hot spots derived from these abnormal operating conditions.

Finally, the estimated equivalent model is used to predict the energy produced by the PV array based on weather forecasts. It is confirmed that the predictions based on estimated values are better than those obtained using baseline values for the model parameters, since they do not take into account possible manufacturing differences among the panels in an array or variations of the panel temperatures.

Incorporating an equivalent dynamic model of a PV array into power system planning and operation enables utilities to better manage the integration of renewable energy into the grid. By more accurately predicting the behavior of the PV array, utilities can optimize the dispatching and scheduling of generation and storage resources, reducing the costs and increasing the reliability.

References

[1] J. Zhao, C. Wan, Z. Xu *et al*., "Impacts of large-scale photovoltaic generation penetration on power system spinning reserve allocation" in *Proceedings of 2016 IEEE PES General Meeting*, Boston, USA, Jul. 2016, pp. 1-5.

[2] R. Nasrin, M. Hasanuzzaman, and N. A. Rahim, "Effect of high irradiation on photovoltaic power and energy," *International Journal of Energy Research*, vol. 42, no. 3, pp. 1115-1131, Mar. 2018.

[3] T. Kozak, W. Marańda, A. Napieralski *et al*., "Influence of ambient temperature on the amount of electric energy produced by solar modules," in *Proceedings of the 16th International Conference – Mixed Design of Integrated Circuits and Systems*, Lodz, Poland, Jun. 2009, pp. 351-354.

[4] S. Sharma, D. K. Vishwakarma, P. Bhardwaj *et al*., "Effects of maintenance on performance of grid connected rooftop solar PV module system," *International Journal of Recent Trends in Engineering and Research*, vol. 4, no. 1, pp. 190-196, Jan. 2018.

[5] A. R. Jordehi, "Parameter estimation of solar photovoltaic (PV) cells: a review," *Renewable and Sustainable Energy Reviews*, vol. 61, pp. 354-371, Aug. 2016.

[6] J. Bai, S. Liu, Y. Hao *et al*., "Development of a new compound method to extract the five parameters of PV modules," *Energy Conversion and Management*, vol. 79, pp. 294-303, Mar. 2014.

[7] O. Mares, M. Paulescu, and V. Badescu, "A simple but accurate procedure for solving the five-parameter model," *Energy Conversion and Management*, vol. 105, pp. 139-148, Nov. 2015.

[8] D. Oliva, E. Cuevas, and G. Pajares, "Parameter identification of solar cells using artificial bee colony optimization," *Energy*, vol. 72, pp. 93-102, Aug. 2014.

[9] A. Askarzadeh and A. Rezazadeh, "Artificial bee swarm optimization algorithm for parameters identification of solar cell models," *Applied Energy*, vol. 102, pp. 943-949, Feb. 2013.

[10] K. Ishaque and Z. Salam, "An improved modeling method to determine the model parameters of photovoltaic (PV) modules using differential evolution (DE)," *Solar Energy*, vol. 85, no. 9, pp. 2349-2359, Sept. 2011.

[11] Z. Huang, K. Schneider, and J. Nieplocha, "Feasibility studies of applying Kalman Filter techniques to power system dynamic state estimation," in *Proceeding of 2007 International Power Engineering Conference (IPEC)*, Singapore, Dec. 2007, pp. 376-382.

[12] M. A. González-Cagigal, J. A. Rosendo-Macías, and A. Gómez-Expósito, "Parameter estimation of fully regulated synchronous generators using unscented Kalman filters," *Electric Power Systems Research*, vol. 168, pp. 210-217, Mar. 2019.

[13] A. Rouhani and A. Abur, "Constrained iterated unscented Kalman filter for dynamic state and parameter estimation," *IEEE Transactions on Power Systems*, vol. 33, no. 3, pp. 2404-2414, May 2018.

[14] N. Zhou, D. Meng, Z. Huang *et al*., "Dynamic state estimation of a synchronous machine using PMU data: a comparative study," in *Proceeding of 2015 IEEE PES General Meeting*, Denver, USA, Jul. 2015, pp. 1-6.

[15] M. Á. González-Cagigal, J. A. Rosendo-Macías, and A. Gómez-Expósito, "State and parameter estimation of photovoltaic modules using unscented Kalman filters," *Renewable Energy and Power Quality Journal*, vol. 20, pp. 126-131, Sept. 2022.

[16] D. Simon, *Optimal State Estimation: Kalman, H-infinity, and Nonlinear Approaches*. New York: Wiley, 2006.
[17] E. A. Wan and R. V. D. Merwe, "The unscented Kalman filter for nonlinear estimation," in *Proceedings of the IEEE 2000 Adaptive Systems for Signal Processing*, *Communications*, *and Control Symposium*, Lake Louise, Canada, Oct. 2000, pp. 153-158.
[18] K. C. Kong, M. B. Mamat, M. Z. Ibrahim *et al*., "New approach on mathematical modeling of photovoltaic solar panel," *Applied Mathematical Sciences*, vol. 6, pp. 381-401, Jan. 2012.
[19] B. Tuncel, T. Ozden, R. S. Balog *et al*., "Dynamic thermal modelling of PV performance and effect of heat capacity on the module temperature," *Case Studies in Thermal Engineering*, vol. 22, p. 100754, Dec. 2020.
[20] R. Santbergen and R. J. C. van Zolingen, "The absorption factor of crystalline silicon PV cells: a numerical and experimental study," *Solar Energy Materials and Solar Cells*, vol. 92, no. 4, pp. 432-444, Apr. 2008.
[21] H. G. Aghamolki, Z. Miao, L. Fan *et al*., "Identification of synchronous generator model with frequency control using unscented Kalman filter," *Electric Power Systems Research*, vol. 126, pp. 45-55, Sept. 2015.
[22] H. W. Sorenson and A. R. Stubberud, "Non-linear filtering by approximation of the a posteriori density," *International Journal of Control*, vol. 8, no. 1, pp. 33-51, Jul. 1968.
[23] W. Squire and G. Trapp, "Using complex variables to estimate derivatives of real functions," *SIAM Review*, vol. 40, no. 1, pp. 110-112, Mar. 1998.
[24] Z. Fan, S. Li, H. Cheng *et al*., "Perturb and observe MPPT algorithm of photovoltaic system: a review," in *Proceedings of 2021 33rd Chinese Control and Decision Conference*, Kunming, China, May 2021, pp. 1413-1418.
[25] AGT. (2023, Mar.). Advanced green technologies. [Online]. Available: https://www.agt.com/services
[26] J. H. Kim, S. Y. Park, Y. R. Kim *et al*., "Analysis of scaling parameters of the batch unscented transformation for precision orbit determination using satellite laser ranging data," *Journal of Astronomy and Space Sciences*, vol. 28, no. 3, pp. 183-192, Sept. 2011.
[27] J. A. Macias and A. Gomez, "Self-tuning of Kalman filters for harmonic computation," *IEEE Transactions on Power Delivery*, vol. 21, no. 1, pp. 501-503, Jan. 2006.

M. A. González-Cagigal received the Industrial Engineer, M.S., and Ph.D. degrees from the University of Seville, Seville, Spain, in 2017, 2019, and 2021, respectively. He is currently with the Department of Electrical Engineering, University of Seville, where he is currently an Assistant Professor. His research interests include dynamic state estimation and operation of electric power systems.

José A. Rosendo-Macías received the Electrical Engineering and Ph.D. degrees from the University of Seville, Seville, Spain, in 1992 and 1997, respectively. Since 1992, he has been with the Department of Electrical Engineering, University of Seville, where he is currently a Professor. His research interests include dynamic state estimation, digital signal processing, digital relaying, and distribution reliability.

A. Gómez-Expósito received the Ph. D. degree in electrical engineering from the University of Seville, Seville, Spain, in 1985. He is currently the Endesa Red Industrial Chair Professor with the University of Seville. His research interests include optimal power system operation, state estimation, digital signal processing, and control of flexible AC transmission system devices.